Two-component fluorescent semiconducting hydrogel from NDI-appended peptide with long chain amines: Variation of thermal and mechanical strength of gels

Article *in* Langmuir · November 2016

DOI: 10.1021/acs.langmuir.6b02727

CITATIONS
41

READS
389

5 authors, including:

Nibedita Nandi
University of Freiburg
15 PUBLICATIONS **493** CITATIONS
SEE PROFILE

Shibaji Basak
Università degli Studi di Trento
21 PUBLICATIONS **1,016** CITATIONS
SEE PROFILE

Steven Kirkham
University of Reading
11 PUBLICATIONS **303** CITATIONS
SEE PROFILE

Ian W Hamley
University of Reading
559 PUBLICATIONS **25,805** CITATIONS
SEE PROFILE

LANGMUIR

Article

pubs.acs.org/Langmuir

Two-Component Fluorescent-Semiconducting Hydrogel from Naphthalene Diimide-Appended Peptide with Long-Chain Amines: Variation in Thermal and Mechanical Strengths of Gels

Nibedita Nandi,[†] Shibaji Basak,[†] Steven Kirkham,[‡] Ian W. Hamley,[‡] and Arindam Banerjee*[,†]

[†]Department of Biological Chemistry, Indian Association for the Cultivation of Science, Jadavpur, Kolkata 700032, India

[‡]Department of Chemistry, University of Reading, Whitenights, Reading RG6 6AD, U.K.

Supporting Information

ABSTRACT: Two-component fluorescent hydrogels have been discovered, containing the mixtures of naphthalene diimide (NDI)-conjugated peptide-functionalized bola-amphiphile and primary amines with long alkyl chains at physiological pH 7.46. The aggregation-induced enhanced emission associated with an NDI-appended peptide in aqueous medium is rare, as water is known to be a good quencher of fluorescence. In this study, an NDI-containing gelator peptide forms a highly fluorescent aggregate in aqueous medium. Absorption and emission spectroscopic techniques reveal the formation of J-aggregates among the chromophoric moieties in their aggregated state in aqueous medium. However, this NDI-containing peptide does not form any gel in aqueous medium. In the presence of the primary amines with long alkyl chains in the buffer solution, it forms two-component fluorescent hydrogels exhibiting bright yellow fluorescence under a UV lamp (365 nm). Probably, the acid−amine interaction between the amines and the bola-amphiphile triggers the gel formation, as evident from Fourier transform infrared data, indicating the presence of a carboxylate group ($-COO^-$) and an ammonium species (NH_3^+) in the coassembled two-component gel system. Low- and wide-angle powder X-ray diffraction and small-angle X-ray scattering further support the fact that the coassembled state in the gel form is produced by the supramolecular interaction between the NDI-based bola-amphiphile and the long-chain amines. Field-emission scanning electron microscopy and high-resolution transmission electron microscopy images reveal that the π-conjugated coassembled hydrogels exhibit nanofibrillar network morphologies. Interestingly, the coassembled hydrogels exhibit an enhanced fluorescence emission, excited-state lifetime, and quantum yield when compared with those of the NDI-containing amphiphile alone in its self-assembled state in aqueous medium. Moreover, the thermal stability and mechanical strength of these gels have been successfully tuned by varying the alkyl chain length of the corresponding amine. Moreover, these NDI−peptide-conjugated soft materials exhibit semiconducting behavior in their respective coassembled states. This holds future promise to use these peptide-appended NDI-based coassembled soft materials for applications in optoelectronic and other devices.

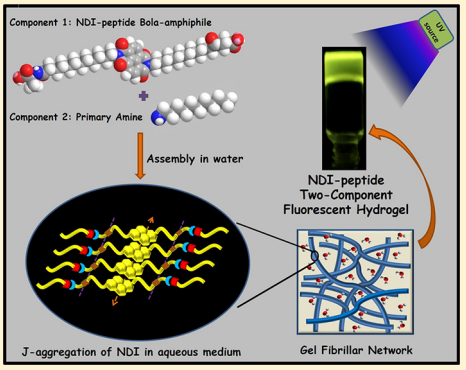

INTRODUCTION

Supramolecular soft materials[1−10] have become a rapidly expanding area in current research for the last few years. Among these soft materials, low-molecular-weight hydrogelators[11−16] are currently finding potential applications in drug delivery, tissue engineering, biosensing, and in other-related fields.[17−26] Most of these gels are obtained from a single-component gelator molecule in aqueous medium. There are several examples of two-component gels[27−29] that provide better diversity and tunability when compared with that of single-component gels. In these cases, the gelation property as well as the thermal and mechanical properties can also be easily controlled by changing the molar ratio of these two components or by varying one of these two components. This offers great promise to design and construct new supramolecular soft materials with structural diversity and tunable functional properties.

Over the past two decades, significant efforts have been devoted to understand the structure−function relationship of organic π-conjugated n-type semiconducting material building blocks owing to their various applications in organic electronic devices such as in photovoltaics, field-effect transistors, and fluorescent bioprobes.[30−38] Among several π-conjugated organic building blocks, molecular planarity, high π-acidity, and their characteristic photophysical behavior made NDIs an important candidate when compared with the higher analogue of rylene dyes in supramolecular research.[39−42] Recently, naphthalene diimide (NDI)−peptide conjugates have been proven advantageous to make new functional supramolecular soft materials with interesting applications because of their

Received: July 22, 2016
Revised: November 9, 2016
Published: November 9, 2016

DOI: 10.1021/acs.langmuir.6b02727
Langmuir 2016, 32, 13226−13233

ability to self-assemble using various noncovalent interactions including $\pi-\pi$ interactions, van der Waals interactions, hydrogen-bonding interactions, and so forth.[43−45] Because of their very weakly fluorescent behavior, NDIs have a limited capacity to exhibit good optical properties in their monomeric states.[46] However, the supramolecular assembly of the NDI-based systems has been studied with great interest because of their interesting photophysical characteristics, such as J-aggregation, excimer emission, aggregation-induced enhanced emission (AIEE), and so forth. AIEE is an effect of the particular assembly of the NDI-based system, and the aggregated species (generally the J-aggregate) exhibits enhanced emission compared with the molecules in their respective monomeric states.[47−51] However, these organic π-conjugated molecules (rylene dyes) generally show non-fluorescent behavior in water because of the aggregation-caused quenching phenomena.[52] Because of the reduction in photoluminescence (PL) efficiency and intrinsic hydrophobicity of the aromatic core, the optical study of the NDI-derivatives in an aqueous environment has been limited.[43] Several previous studies have been directed to explore the assembly of NDI derivatives in aqueous medium,[53,54] and there are only a few reports on the assembly of NDI/peptide-conjugated soft materials[55,56] in aqueous medium. Parquette and co-workers have reported the formation of an NDI−dilysine peptide-based self-supporting hydrogel.[57] There are a few reports on the formation of NDI-based hydrogels under physiological conditions and on the hydrogelation of NDI/amino acid conjugates.[58−60] However, none of these examples include the self-assembly of an NDI-appended peptide that not only forms two-component hydrogels with long-chain amines but also promotes aggregation-induced fluorescence in an aqueous medium. To the best of our knowledge, this is the first example of an NDI-appended peptide-based two-component hydrogel (with long-chain alkyl amines) that has shown aggregation-induced fluorescence in an aqueous medium. The merit of this two-component system is to tune the thermal, mechanical, and photophysical properties of the assembled NDI system by varying the chain length of the alkyl amine. Interestingly, fluorescence properties (i.e., fluorescence intensity, quantum yield, and fluorescence lifetime in the excited state) of this NDI-based moiety are remarkably changed in the two-component gel system compared with that of the self-assembly of NDI-based peptide alone in water. Encouraged by the intriguing photophysical properties of NDI moieties, we are curious to study the effect of the self-assembly of the chromophoric moiety on the electrical conductance of NDI-based functional soft materials.

In this study, utilizing a rational design, we report an unprecedented two-component fluorescent hydrogel system based on an NDI-conjugated dipeptide-functionalized bola-amphiphile **P** and long-chain primary alkyl amines in physiological phosphate buffer solution at pH 7.46 (Figure 1). The NDI-based bola-amphiphile has been chosen in such a way that it can be self-associated utilizing $\pi-\pi$ interactions involving the NDI core, hydrogen-bonding interactions using the intervening amide (−CONH) moieties, van der Waals interactions from the intervening polymethylene units of the NDI-based peptide and from the long fatty acyl chain, and electrostatic interactions between the carboxylate ($-COO^-$) group and ammonium ($-NH_3^+$) species of the long-chain amine. This newly formed hydrogel is fluorescent and emits a bright greenish-yellow color on illumination under the UV lamp (365 nm).

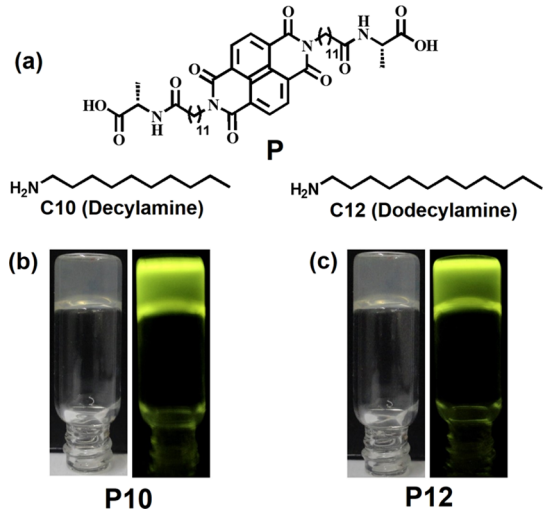

Figure 1. (a) Chemical structures of the peptide (**P**) and amines decylamine (**C10**) and dodecylamine (**C12**). (b and c) Photographs of two-component hydrogels P10 (**P** with **C10**) and P12 (**P** with **C12**) at a 1:2 molar ratio of peptide/amine in daylight (left side) and under UV lamp (right side) (365 nm), respectively.

EXPERIMENTAL SECTION

L-Alanine (L-Ala), 12-aminododecanoic acid, and 1,4,5,8-naphthalenetetracarboxylic dianhydride were purchased from Aldrich. Decylamine (**C10**), dodecylamine (**C12**), 1-hydroxybenzotriazole, *N*,*N*′-dicyclohexylcarbodiimide, and all solvents were purchased from SRL, India. Details on the synthetic procedures of gelator peptide, instrumentation, and spectroscopic analysis are given in the Supporting Information.

RESULTS AND DISCUSSION

Gelation Study. The NDI-based peptide **P** did not form gels by itself in the phosphate buffer solution at pH 7.46; however, the combination of both peptide **P** and one of these long-chain amines (**C10** or **C12**) provided a two-component hydrogel. The gel is stable in the pH range 7.0−8.5, and it is also thermoreversible in nature. The gelation properties of this two-component system were studied in the buffer solution by dissolving peptide **P** with each amine by changing their proportions. The stable molar ratio of peptide **P** and amines was found to be 1:2. Interestingly, any coassembly with the molar ratio of peptide **P**/amine = 1:1 did not form stable hydrogels in the buffer solution (pH 7.46), but a viscous solution was observed (Figure S1). Only when the molar ratio was increased to 1:2, a transparent hydrogel was obtained (Figure 1). For the other combinations such as peptide **P**/amine = 1:3 and 1:4, the systems were also unable to form any gel in the buffer solution at pH 7.46 (Figure S1). The gelation ability of peptide **P** was examined using different primary long-chain amines such as *n*-octylamine, *n*-decylamine, *n*-dodecylamine, and *n*-tetradecylamine. It is worth noting that the gelation occurred only for decylamine and dodecylamine. However, the other two long-chain amines failed to form such gels under the same conditions. The mixture of peptide **P** with *n*-octylamine formed a soluble aggregate, whereas the mixture obtained from tetradecylamine was very hard to dissolve and gave a precipitate under the same conditions. This fact shows that the gel formation is dependent on the chain length of the

DOI: 10.1021/acs.langmuir.6b02727
Langmuir 2016, 32, 13226−13233

corresponding alkyl amine. The gelation properties of the two-component systems were also studied with different amines including secondary amines, tertiary amines, cyclic amines, and aromatic amines, but the gelation occurred only with long-chain aliphatic primary amines. In this paper, a detailed study of the gel properties for decylamine containing the two-component aggregate (P10 hydrogel) (Figure 1b) and dodecylamine containing the two-component aggregate (P12 hydrogel) (Figure 1c) is included, at 1:2 ratio of peptide **P** and the corresponding amine. Minimum gelation concentration (MGC) values were found to be 0.07% (w/v) for gel P10 and 0.04% (w/v) for gel P12. The MGC values were calculated with respect to peptide **P**. The gel melting temperatures (T_{gel}) of these hydrogels were found to be 40 and 47 °C for gels P10 and P12, respectively, at 1.25 mM concentration. This indicates the modulation of thermal stability by the variation in the alkyl chain length of the corresponding amine in two-component hydrogels (Table S1). This type of trend was also previously observed in two-component dendritic organogels.[28]

Morphological Study. To obtain a clear overview of the morphological features of the two-component hydrogel system, high-resolution transmission electron microscopy (HR-TEM) and field-emission scanning electron microscopy (FE-SEM) experiments were carried out. The HR-TEM images (Figure 2a,b) and FE-SEM images (Figure 2c,d) of the xerogels

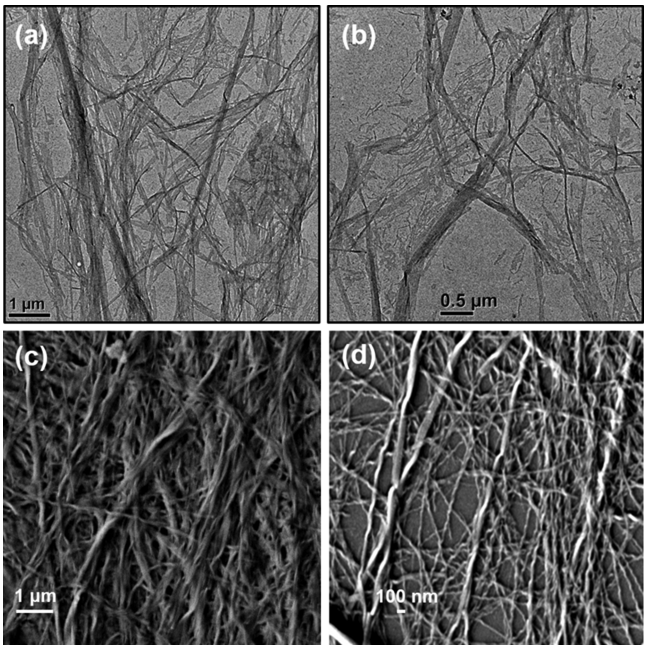

Figure 2. (a and b) HR-TEM and (c and d) FE-SEM images of the xerogels obtained from hydrogels P10 and P12 (at a 1:2 molar ratio of peptide/amine).

(obtained from hydrogels P10 and P12 at pH 7.46) show the nanofibrillar morphologies for both of these hydrogels. These images reveal that these aggregates are composed of numerous nanofibers that are elongated to several micrometers in length. These nanofibres are entangled with each other in a long range to form a nanofibrillar gel network structure that entraps the water molecules to form a self-supported gel. Careful inspection of the FE-SEM image reveals that the nanofibres are 50−60 nm in width and twisted in nature, although some of them are bundled up to form fibers with relatively more thickness. The different strategies for the preparation of samples for FE-SEM and HR-TEM studies may be the reason for the difference in the appearance of these fibers in different morphological studies.

Rheological Study. To obtain the fundamental mechanical properties and flow behavior of the two-component hydrogels, rheological experiments have been carried out at a constant oscillatory frequency of 1 Hz at room temperature (25 °C). In a frequency sweep rheological experiment presented in Figure 3,

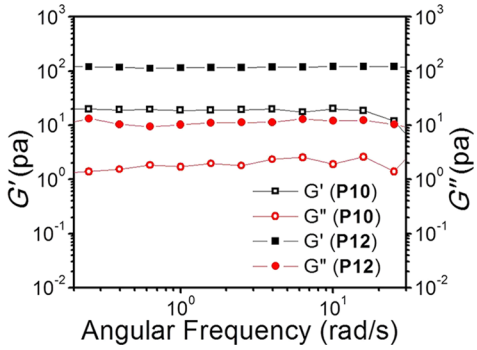

Figure 3. Log−log plot of storage modulus (G') and loss modulus (G'') vs angular frequency of hydrogels P10 and P12 (at a 1:2 molar ratio of peptide/amine) at 2.5 mM concentration.

it is observed that the storage modulus (G') values are higher than the loss modulus (G'') values for both hydrogels P10 and P12 (at a 1:2 molar ratio of peptide/amine) at 2.5 mM concentration of the respective peptide. In these experiments, G' and G'' did not cross each other ($G' > G''$) and they are found to be almost parallel to the angular frequency applied throughout the experimental region. These observations suggest the formation of a soft "solid-like" gel phase. It is evident from the plot that the coassembled hydrogel P12 with longer alkyl chain amines has a 6-fold increase in the G' and G'' values when compared with those of hydrogel P10 with relatively shorter alkyl chain amines. The longer aliphatic chain of **C12** probably allows the assembly of bola-amphiphile **P** with **C12** in a more sterically favorable conformation than that with **C10**, and this makes hydrogel P12 more robust than hydrogel P10.[28] Rheological studies were performed in other two concentrations (2 and 3 mM) to explore the possibility of variance in storage and loss moduli of these coassembled gels P10 and P12 (Figure S5). It was found that both storage and loss moduli of these two gels were dependent on the concentration.

Time-Correlated Single-Photon-Counting Study. Time-correlated single-photon-counting (TCSPC) experiments were performed to get insights into the aggregation-induced change in the emission properties of peptide **P**. In tetrahydrofuran (THF), the excitation monochromator was set to 340 nm and the emission was recorded at 410 nm for peptide **P**. Short-lived decay was noticed with an average lifetime of 721 ps, arising for the monomeric NDI fluorophore because of the fast intersystem crossing to the close-lying triplet state. Similar experiments were performed for peptide **P** in aqueous medium (buffer solution of pH 7.46) with an excitation at 340 nm, and the emission was monitored at 527 nm. At 527 nm, a triexponential decay was observed with a substantially longer average lifetime of 1.99 ns (Figure 4). The concentration of peptide **P** was kept constant at 0.05 mM

DOI: 10.1021/acs.langmuir.6b02727
Langmuir 2016, 32, 13226−13233

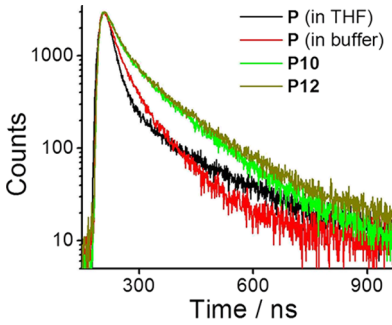

Figure 4. TCSPC decay profiles obtained from peptide **P** (in THF and buffer solution), two-component aggregates P10 and P12 (at a 1:2 molar ratio of peptide/amine) at 0.05 mM concentration.

throughout the experiment. For the experiments conducted using coassembled aggregated systems P10 and P12, on excitation at 340 nm, the emissions were recorded at 529 and 531 nm, respectively. In these cases, the resultant decay profiles also show a triexponential decay with a substantially longer average lifetime of 3.18 and 3.33 ns. These observations also suggest that the excited-state complexes of P10 and P12 are significantly more stable than that of peptide **P** alone in aqueous medium. Notably, the quantum yield of peptide **P** was found to be 3.6% in aqueous medium using quinine sulfate as a reference dye. However, the quantum yields for the two-component aggregated systems P10 and P12 were found to be 4.2 and 5.4%, respectively, using the same reference dye (quinine sulfate). The detailed data for the TCSPC study and quantum yield are tabulated in Table 1. These observations

Table 1. Quantum Yield (Φ) and Fluorescence Lifetime in Excited State (with Time Components τ_1, τ_2, and τ_3) Obtained from TCSPC Measurements of Peptide P (in THF and Buffer Solution) and for Two-Component Aggregates P10 and P12 (at a 1:2 Molar Ratio of Peptide/Amine)

sample	quantum yield Φ (%)	τ_1 (%) ns	τ_2 (%) ns	τ_3 (%) ns	average lifetime τ_{avg} (%) ns
peptide **P** (in THF)		0.046 (99.0)	0.011 (0.8)	0.015 (0.2)	0.072
peptide **P** (in water)	3.6	0.910 (73.5)	0.936 (25.2)	0.149 (1.31)	1.99
P10	4.2	0.961 (23.2)	1.295 (15.5)	0.922 (61.3)	3.18
P12	5.4	1.036 (66.9)	1.703 (28.5)	0.596 (4.6)	3.33

may be due to the fact that the aggregation of the coassembled system is more profound in the two-component aggregated system than the aggregation of the self-assembled NDI-based peptide **P** alone in aqueous medium. Moreover, the coassembled aggregate P12 with comparatively long alkyl chain amines induces the assembly of the NDI fluorophore more than the aggregate P10 with an amine with the shorter alkyl chain length.

Spectroscopic Study. To get an overview about the aggregation pattern of the two-component coassembled system, a photophysical study was performed in the self-associated state of peptide **P**. For this purpose, UV−vis spectroscopic study of peptide **P** was performed to examine the aggregation pattern from the monomeric chromophore to the aggregated state by changing the solvent from THF to buffer solution (pH 7.46) and then by systematically increasing the amine concentration in the system. The concentration of peptide **P** was kept constant at 0.005 mM throughout the experiment. In Figure 5,

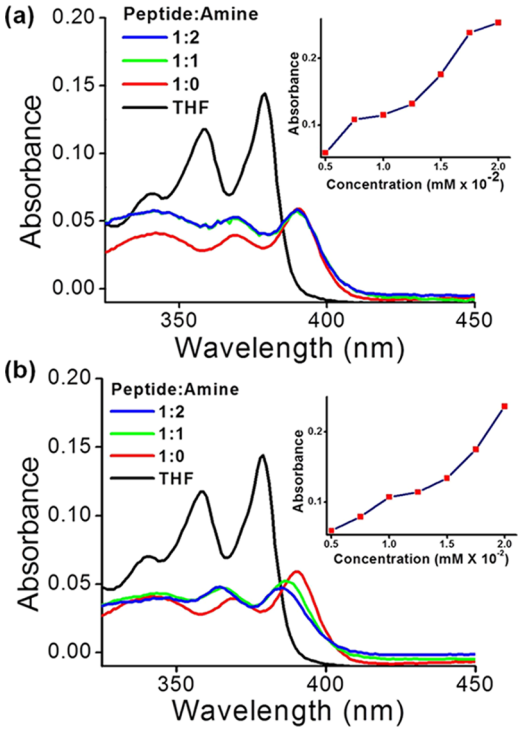

Figure 5. (a) Absorption spectra obtained from monomeric (in THF) and aggregated states (in buffer solution) of peptide **P** and two-component P10 aggregates (at 1:1 and 1:2 molar ratios of peptide/amine). (b) Absorption spectra obtained from monomeric (in THF) and aggregated states (in buffer solution) of peptide **P** and two-component P12 aggregates (at 1:1 and 1:2 molar ratios of peptide/amine). Insets of figures: absorbance at 389 nm with the increasing concentration of P10 and P12 aggregates at a 1:2 molar ratio of peptide/amine. The concentration of peptide **P** was 0.005 mM for all of these cases.

peptide **P** shows well-resolved sharp absorption bands in the range of 300−400 nm in THF. This arises due to a $\pi-\pi^*$ transition along the long axis of the chromophore in the monomeric state. In THF, peaks appeared at 379 and 359 nm with a shoulder around 340 nm. However, when the solvent system was changed from THF to buffer solution, peptide **P** tends to form aggregates in aqueous medium. This is evident from the bathochromic shift (11 nm) and about a 60% decrease in the lowest-energy absorption peak (379 nm), as shown in Figure 5. For the two-component complex P10 (at a 1:2 molar ratio of **P** and **C10**), a similar type of change in peak position was observed that shows a bathochromic shift of 11 nm and a 59% decrease in absorbance for the lowest energy peak (Figure 5a). However, the peak position for P12 aggregate was slightly different from that for P10 aggregate. For P12 aggregate (at a 1:2 molar ratio of **P** and **C12**), there was a 6 nm red shift and a 68% decrease in the absorbance upon aggregation (Figure 5b). However, at a 1:1 molar ratio of peptide **P** and **C12**, an 8 nm red shift and a 64% decrease in absorbance of the lowest energy peak was observed. The red shift and remarkable decrease in the lowest-energy absorption peak in all aqueous media suggest that the J-aggregated $\pi-\pi$ stacking is present in the aggregated state of the chromophore.[42,43] The concentration-dependent UV−vis spectroscopy were performed at a 1:2 molar ratio of

DOI: 10.1021/acs.langmuir.6b02727
Langmuir 2016, 32, 13226−13233

peptide/amine for both P10 and P12 aggregated systems (Figure S6) at a 0.005 mM concentration of peptide **P**. The peaks appeared at the similar position (389 nm), and the absorption was observed with a regular increase with increase in the concentration of peptide **P** (Figure 5, inset).

To get more insight into the optical property of the two-component coassembled system, a PL study was carried out for peptide **P** in both THF and buffer solution (pH 7.46) at 0.5 mM concentration. The solvent change from THF to buffer solution can significantly alter the aggregation pattern followed by a drastic change in the fluorescence behavior. In THF, a very small emission band was observed at 410 nm because of the nonaggregated state of the chromophore at an excitation of 340 nm. It exhibits a very weak emission in THF but emits a strong greenish-yellow fluorescence with more than a 300-fold increase in the emissive intensity upon aggregation in the buffer solution (pH 7.46). For this case, the emission spectra showed two prominent bands centered at 460 and 550 nm, as apparent in Figure 6a,b. An intense peak around 527 nm

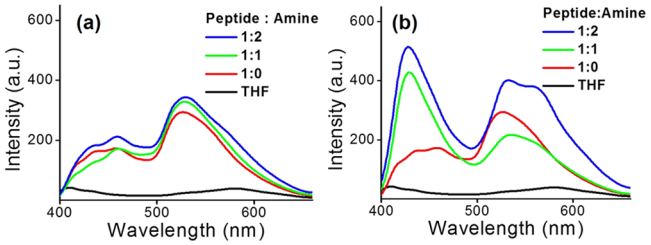

Figure 6. (a) Emission spectra obtained from monomeric (in THF) and aggregated states (in buffer solution) of peptide **P** and two-component P10 aggregates (at 1:1 and 1:2 molar ratios of peptide/amine) upon excitation at 340 nm. (b) Emission spectra obtained from monomeric (in THF) and aggregated states (in buffer solution) of peptide **P** and two-component P12 aggregates (at 1:1 and 1:2 molar ratios of peptide/amine) upon excitation at 340 nm. The concentration of peptide **P** was 0.5 mM for all of these cases.

accompanied by a broad emission band around 435−460 nm suggests the AIEE of NDI-based peptide **P** in aqueous medium. After the addition of **C10** to make a 1:1 proportional mixture with peptide **P**, the peak intensity around 529 nm was gradually increased (Figure 6a). At a 1:2 molar ratio of **P** and **C10**, this peak intensity was further increased. The PL spectrum of this two-component aggregate P12 is quite different from that of the aggregate P10. At a 1:1 molar ratio of **P** and **C12**, an enhancement of the peak intensity was noticed around 430 nm accompanied by a broad peak around 529 nm (Figure 6b). The intensity of these peaks gradually increased while changing the molar ratio from 1:1 to 1:2. In addition to that, a broad emission band around 530−560 nm was also noticed for P12 aggregate at a 1:2 molar ratio of peptide **P**/amine. Therefore, the two-component coassembled systems P10 and P12 emit greenish-yellow fluorescence under the UV lamp (365 nm).

Powder X-Ray Diffraction and Small-Angle X-Ray Scattering Studies. The internal packing arrangement of the self-assembled hydrogel was investigated using both wide-angle and low-angle powder X-ray diffractions (PXRDs) for the xerogels obtained from hydrogels P10 and P12 at the molar ratio 1:2 of peptide **P** and amine. In the low-angle region (Figure 7a,c), distinct peaks at 2θ = 2.2° (d = 40.53 Å) and 1.81° (d = 48.88 Å) were observed for P10 and P12, respectively. These values matched well with the calculated molecular length (44.28 Å) of peptide **P** on its own. In the

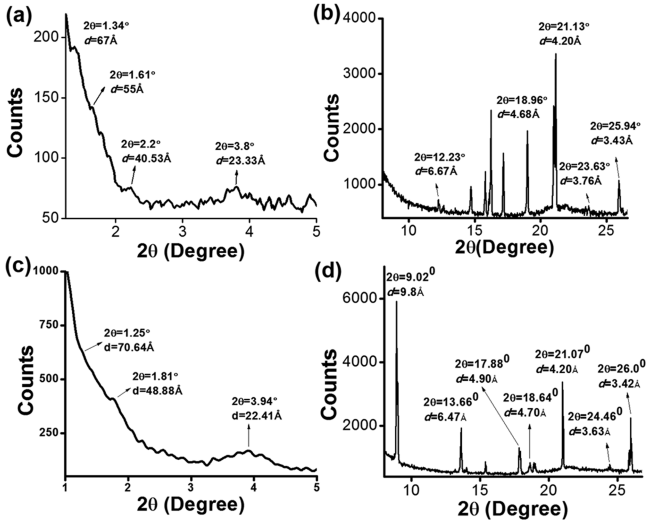

Figure 7. (a and c) Low-angle PXRD and (b and d) wide-angle PXRD patterns obtained from the xerogels of hydrogels P10 and P12 (at a 1:2 molar ratio of peptide/amine).

small-angle X-ray scattering (SAXS) data for hydrogel P12, a peak appeared corresponding to a d-spacing value of 43.47 Å, also in good agreement with the length of the molecule **P** (Figure S7). A broad peak corresponding to a d-spacing value of 67 Å (2θ = 1.34°) and 70.64 Å (2θ = 1.25°) was observed for P10 and P12, respectively, from low-angle PXRD, and for both cases, these values are close to the calculated total length of peptide **P** (74.84 Å) with two amines (**C10** and **C12**) in the assembled structure as depicted in a tentative model in Figure 8. The reflection peaks appeared at 2θ = 3.8° (d = 23.33 Å) and 3.94° (d = 22.41 Å) for P10 and P12, respectively, which correspond to the second-order peaks from a structure with a spacing equal to the molecular length of **P**. In the wide-angle region (Figure 7b,d), the peaks are observed at 2θ = 9.02° and 18.64°, which correspond to the d-spacing value of 9.8 and 4.7 Å, respectively, for P12 indicating a sheet-like assembly in the gel state.[61] A peak at 2θ = 25.94° with a d-spacing value of 3.43 Å was observed for P10, which is the characteristic peak for the $\pi-\pi$ stacking of the NDI core. A similar characteristic peak also appeared at 2θ = 26.0° with the corresponding d-spacing value of 3.42 Å for P12.

FTIR Analysis. In the solid state of peptide **P**, a characteristic peak due to C═O stretching frequency corresponding to carboxylic acid (−COOH) was observed at 1707 cm^{-1}, whereas, in the xerogel state, the intensity of this peak is diminished (Figure 9). In the gel state, peaks due to the C═O stretch band of carboxylate anions appeared at 1584 and 1392 cm^{-1} for hydrogel P10. For hydrogel P12, these peaks are at 1582 and 1408 cm^{-1}. This observation suggests that in the gel state, the gelator molecules are present in the carboxylate ($-COO^-$) form. The presence of peaks corresponding to the N−H stretching frequency at 3307 and 3308 cm^{-1} and the amide carbonyl stretching frequency at 1640 and 1646 cm^{-1} for P10 and P12, respectively, indicate the hydrogen bond formation in the gel state. The peaks at 3414 and 3418 cm^{-1} can be assigned as the NH-stretching frequency of ammonium species of the amine part of the two-component gels in their assembled state.

Current−Voltage Study. Although there are several reports of semiconducting behavior of NDI-based soft materials mainly obtained from organic solvents,[62] a water-processable

DOI: 10.1021/acs.langmuir.6b02727
Langmuir 2016, 32, 13226−13233

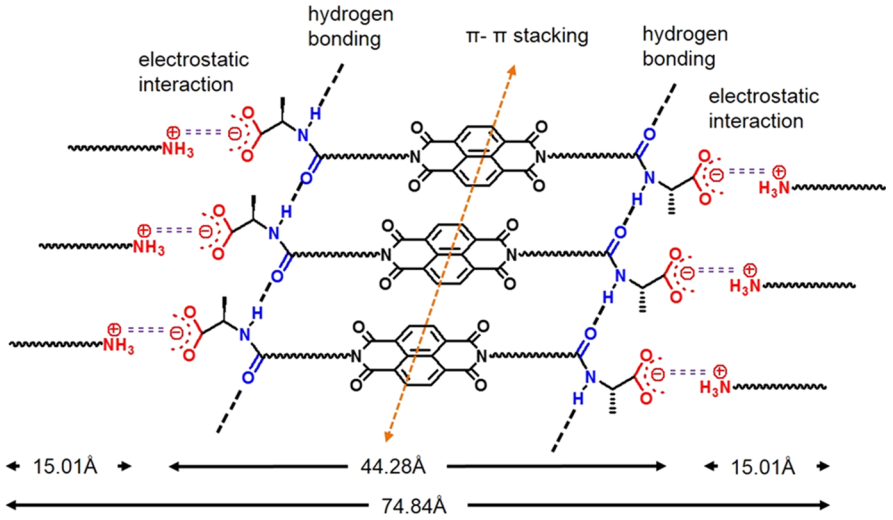

Figure 8. Tentative model for the molecular packing arrangements among the gelator molecules in the two-component coassembled system obtained from Fourier transform infrared (FTIR), PXRD, and SAXS data. The molecular length of dodecylamine (**C12**) has been used to calculate the total molecular length in the two-component coassembled structure.

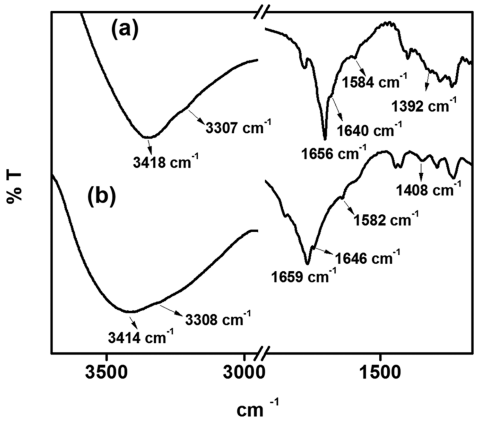

Figure 9. FTIR spectra of the xerogels obtained from hydrogels (a) P10 and (b) P12 (at a 1:2 molar ratio of peptide/amine).

NDI-based soft material that shows semiconducting behavior is yet to be explored. Therefore, in this study, the bulk electrical conductivity of peptide-containing NDI materials with the corresponding amines in their coassembled states has been measured by the current−voltage study. It is evident from the *I*−*V* plot (Figure 10) that the increment of current with respect to the voltage applied follows a linear relationship in the low-voltage region for both P10 and P12 xerogels (at a 1:2 molar ratio of peptide/amine) in their respective coassembled states, confirming the development of ohmic interactions ($V/I = R$). However, in the higher voltage region, the *I*−*V* curves show deviation from the linearity. This indicates the semiconducting nature of these two-component systems. The conductivity of both P10 and P12 xerogels has been calculated to be 5.5−6 × 10^{-6} S cm^{-1}. These observations demonstrate an excellent electrical semiconducting behavior for the two-component NDI-based systems in their xerogel states.

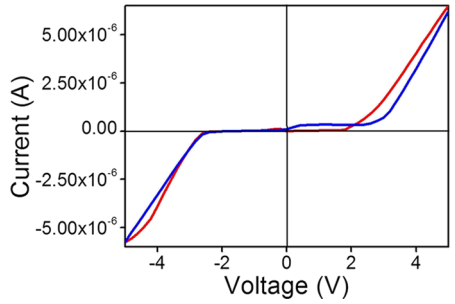

Figure 10. *I*−*V* characteristics shown by the two-component xerogels obtained from hydrogels P10 (blue line) and P12 (red line) at a 1:2 molar ratio of peptide/amine.

CONCLUSIONS

In summary, two-component fluorescent hydrogels have been made from the peptide-appended NDI moiety and long-chain primary amines in aqueous medium. These gels have been thoroughly characterized by FTIR, XRD, SAXS, TEM, and rheological experiments. Interestingly, thermal and mechanical strengths of the gels have been nicely tuned by varying the alkyl chain length of the primary amines. Moreover, these two-component coassembled gels exhibit appreciable semiconducting properties, as evident from their *I*−*V* characteristics. The discovery of NDI-based highly fluorescent two-component new soft materials in an ecofriendly solvent (water) opens up future directions for the development and construction of smart materials for their applications in optoelectronic devices, fluorescence biosensors, and other purposes.

ASSOCIATED CONTENT

Supporting Information

The Supporting Information is available free of charge on the ACS Publications website at DOI: 10.1021/acs.langmuir.6b02727.

Experimental section, instrumentation, gel preparation, synthetic procedures, NMR, MALDI-TOF MS, spectroscopic study, SAXS, and rheological study (PDF)

AUTHOR INFORMATION

Corresponding Author

*E-mail: bcab@iacs.res.in. Fax: (+91)-33-2473-2805.

ORCID

Ian W. Hamley: 0000-0002-4549-0926

DOI: 10.1021/acs.langmuir.6b02727
Langmuir 2016, 32, 13226−13233

Arindam Banerjee: 0000-0002-1309-921X

Notes

The authors declare no competing financial interest.

■ ACKNOWLEDGMENTS

N.N. gratefully acknowledges CSIR, New Delhi, India for the financial assistance. We acknowledge Rumana Parveen, Department of Organic Chemistry, IACS and Department of Biotechnology (DBT), New Delhi (DBT project number: BT/01/CEIB/11/V/13) for allowing us to use the Anton Paar modular compact rheometer (MCR 102) for rheological measurements.

■ REFERENCES

(1) Caruso, M.; Gatto, E.; Placidi, E.; Ballano, G.; Formaggio, F.; Toniolo, C.; Zanuy, D.; Alemán, C.; Venanzi, M. A single-residue substitution inhibits fibrillization of Ala-based pentapeptides. A spectroscopic and molecular dynamics investigation. *Soft Matter* **2014**, *10*, 2508−2519.

(2) Ziserman, L.; Lee, H.-Y.; Raghavan, S. R.; Mor, A.; Danino, D. Unraveling the Mechanism of Nanotube Formation by Chiral Self-Assembly of Amphiphiles. *J. Am. Chem. Soc.* **2011**, *133*, 2511−2517.

(3) Oh, H.; Javvaji, V.; Yaraghi, N. A.; Abezgauz, L.; Danino, D.; Raghavan, S. R. Light-induced transformation of vesicles to micelles and vesicle-gels to sols. *Soft Matter* **2013**, *9*, 11576−11584.

(4) Terech, P.; Dourdain, S.; Bhat, S.; Maitra, U. Self-Assembly of Bile Steroid Analogues: Molecules, Fibers, and Networks. *J. Phys. Chem. B* **2009**, *113*, 8252−8267.

(5) Mallia, V. A.; Weiss, R. G. Correlations between thixotropic and structural properties of molecular gels with crystalline networks. *Soft Matter* **2016**, *12*, 3665−3676.

(6) Feldner, T.; Häring, M.; Saha, S.; Esquena, J.; Banerjee, R.; Díaz, D. D. Supramolecular Metallogel That Imparts Self-Healing Properties to Other Gel Networks. *Chem. Mater.* **2016**, *28*, 3210−3217.

(7) Armelin, E.; Pérez-Madrigal, M. M.; Alemán, C.; Díaz, D. D. Current status and challenges of biohydrogels for applications as supercapacitors and secondary batteries. *J. Mater. Chem. A* **2016**, *4*, 8952−8968.

(8) Adler-Abramovich, L.; Gazit, E. The physical properties of supramolecular peptide assemblies: From building block association to technological applications. *Chem. Soc. Rev.* **2014**, *43*, 6881−6893.

(9) Zhang, L.; Jin, Q.; Liu, M. Enantioselective Recognition by Chiral Supramolecular Gels. *Chem.—Asian J.* **2016**, *11*, 2642−2649.

(10) Maiti, D. K.; Banerjee, A. A Synthetic Amino Acid Residue Containing A New Oligopeptide-Based Photosensitive Fluorescent Organogel. *Chem.—Asian J.* **2013**, *8*, 113−120.

(11) Gupta, J. K.; Adams, D. J.; Berry, N. G. Will it gel? Successful computational prediction of peptide gelators using physicochemical properties and molecular fingerprints. *Chem. Sci.* **2016**, *7*, 4713−4719.

(12) Singh, N.; Conte, M. P.; Ulijn, R. V.; Miravet, J. F.; Escuder, B. Insight into the esterase like activity demonstrated by an imidazole appended self-assembling hydrogelator. *Chem. Commun.* **2015**, *51*, 13213−13216.

(13) Foster, J. A.; Edkins, R. M.; Cameron, G. J.; Colgin, N.; Fucke, K.; Ridgeway, S.; Crawford, A. G.; Marder, T. B.; Beeby, A.; Cobb, S. L.; Steed, J. W. Blending Gelators to Tune Gel Structure and Probe Anion-Induced Disassembly. *Chem.—Eur. J.* **2014**, *20*, 279−291.

(14) Cayuela, A.; Kennedy, S. R.; Soriano, M. L.; Jones, C. D.; Valcárcel, M.; Steed, J. W. Fluorescent carbon dot−molecular salt hydrogels. *Chem. Sci.* **2015**, *6*, 6139−6146.

(15) Weiss, R. G. The Past, Present, and Future of Molecular Gels. What Is the Status of the Field, and Where Is It Going? *J. Am. Chem. Soc.* **2014**, *136*, 7519−7530.

(16) Cardoso, A. Z.; Mears, L. L. E.; Cattoz, B. N.; Griffiths, P. C.; Schweins, R.; Adams, D. J. Linking micellar structures to hydrogelation for salt-triggered dipeptide gelators. *Soft Matter* **2016**, *12*, 3612−3621.

(17) Baral, A.; Basak, S.; Basu, K.; Dehsorkhi, A.; Hamley, I. W.; Banerjee, A. Time-dependent gel to gel transformation of a peptide based supramolecular gelator. *Soft Matter* **2015**, *11*, 4944−4951.

(18) Maity, M.; Sajisha, V. S.; Maitra, U. Hydrogelation of bile acid−peptide conjugates and in situ synthesis of silver and gold nanoparticles in the hydrogel matrix. *RSC Adv.* **2015**, *5*, 90712−90719.

(19) Baral, A.; Roy, S.; Ghosh, S.; Hermida-Merino, D.; Hamley, I. W.; Banerjee, A. A Peptide-Based Mechano-Sensitive, Proteolytically Stable Hydrogel with Remarkable Antibacterial Properties. *Langmuir* **2016**, *32*, 1836−1845.

(20) Zhou, J.; Du, X.; Gao, Y.; Shi, J.; Xu, B. Aromatic−Aromatic Interactions Enhance Interfiber Contacts for Enzymatic Formation of a Spontaneously Aligned Supramolecular Hydrogel. *J. Am. Chem. Soc.* **2014**, *136*, 2970−2973.

(21) Yuan, D.; Du, X.; Shi, J.; Zhou, N.; Zhou, J.; Xu, B. Mixing Biomimetic Heterodimers of Nucleopeptides to Generate Biocompatible and Biostable Supramolecular Hydrogels. *Angew. Chem., Int. Ed.* **2015**, *54*, 5705−5708.

(22) Jung, J. H.; Lee, J. H.; Silverman, J. R.; John, G. Coordination polymer gels with important environmental and biological applications. *Chem. Soc. Rev.* **2013**, *42*, 924−936.

(23) Sun, J. E. P.; Stewart, B.; Litan, A.; Lee, S. J.; Schneider, J. P.; Langhans, S. A.; Pochan, D. J. Sustained release of active chemotherapeutics from injectable-solid β-hairpin peptide hydrogel. *Biomater. Sci.* **2016**, *4*, 839−848.

(24) Knerr, P. J.; Branco, M. C.; Nagarkar, R.; Pochan, D. J.; Schneider, J. P. Heavy metal ion hydrogelation of a self-assembling peptide via cysteinyl chelation. *J. Mater. Chem.* **2012**, *22*, 1352−1357.

(25) Swanekamp, R. J.; Welch, J. J.; Nilsson, B. L. Proteolytic stability of amphipathic peptide hydrogels composed of self-assembled pleated β-sheet or coassembled rippled β-sheet fibrils. *Chem. Commun.* **2014**, *50*, 10133−10136.

(26) da Silva, E. R.; Walter, M. N. M.; Reza, M.; Castelletto, V.; Ruokolainen, J.; Connon, C. J.; Alves, W. A.; Hamley, I. W. Self-Assembled Arginine-Capped Peptide Bolaamphiphile Nanosheets for Cell Culture and Controlled Wettability Surfaces. *Biomacromolecules* **2015**, *16*, 3180−3190.

(27) Liu, Y.; Chen, C.; Wang, T.; Liu, M. Supramolecular Chirality of the Two-Component Supramolecular Copolymer Gels: Who Determines the Handedness? *Langmuir* **2016**, *32*, 322−328.

(28) Hirst, A. R.; Smith, D. K.; Feiters, M. C.; Geurts, H. P. M. Two-Component Dendritic Gel: Effect of Spacer Chain Length on the Supramolecular Chiral Assembly. *Langmuir* **2004**, *20*, 7070−7077.

(29) Hirst, A. R.; Miravet, J. F.; Escuder, B.; Noirez, L.; Castelletto, V.; Hamley, I. W.; Smith, D. K. Self-Assembly of Two-Component Gels: Stoichiometric Control and Component Selection. *Chem.—Eur. J.* **2009**, *15*, 372−379.

(30) Hu, Z.; Pantoş, G. D.; Kuganathan, N.; Arrowsmith, R. L.; Jacobs, R. M. J.; Kociok-Köhn, G.; O'Byrne, J.; Jurkschat, K.; Burgos, P.; Tyrrell, R. M.; Botchway, S. W.; Sanders, J. K. M.; Pascu, S. I. Interactions between Amino Acid-Tagged Naphthalenediimide and Single Walled Carbon Nanotubes for the Design and Construction of New Bioimaging Probes. *Adv. Funct. Mater.* **2012**, *22*, 503−518.

(31) Ryan, S. T. J.; Young, R. M.; Henkelis, J. J.; Hafezi, N.; Vermeulen, N. A.; Hennig, A.; Dale, E. J.; Wu, Y.; Krzyaniak, M. D.; Fox, A.; Nau, W. M.; Wasielewski, M. R.; Stoddart, J. F.; Scherman, O. A. Energy and Electron Transfer Dynamics within a Series of Perylene Diimide/Cyclophane Systems. *J. Am. Chem. Soc.* **2015**, *137*, 15299−15307.

(32) Hou, X.; Ke, C.; Bruns, C. J.; McGonigal, P. R.; Pettman, R. B.; Stoddart, J. F. Tunable solid-state fluorescent materials for supramolecular encryption. *Nat. Commun.* **2015**, *6*, 6884.

(33) Yuan, Z.; Ma, Y.; Geßner, T.; Li, M.; Chen, L.; Eustachi, M.; Weitz, R. T.; Li, C.; Müllen, K. Core-Fluorinated Naphthalene Diimides: Synthesis, Characterization, and Application in n-Type Organic Field-Effect Transistors. *Org. Lett.* **2016**, *18*, 456−459.

(34) Pandeeswar, M.; Govindaraju, T. Engineering molecular self-assembly of perylene diimide through pH-responsive chiroptical switching. *Mol. Syst. Des. Eng.* **2016**, *1*, 202−207.

DOI: 10.1021/acs.langmuir.6b02727
Langmuir 2016, 32, 13226−13233

(35) Babu, S. S.; Praveen, V. K.; Ajayaghosh, A. Functional π-Gelators and Their Applications. *Chem. Rev.* **2014**, *114*, 1973−2129.
(36) Yun, S. W.; Kim, J. H.; Shin, S.; Yang, H.; An, B.-K.; Yang, L.; Park, S. Y. High-Performance n-type Organic Semiconductors: Incorporating Specific Electron-Withdrawing Motifs to Achieve Tight Molecular Stacking and Optimized Energy Levels. *Adv. Mater.* **2012**, *24*, 911−915.
(37) Aparicio, F.; Cherumukkil, S.; Ajayaghosh, A.; Sánchez, L. Color-Tunable Cyano-Substituted Divinylene Arene Luminogens as Fluorescent π-Gelators. *Langmuir* **2016**, *32*, 284−289.
(38) Das, J.; Siram, R. B. K.; Cahen, D.; Rybtchinski, B.; Hodes, G. Thiophene-modified perylenediimide as hole transporting material in hybrid lead bromide perovskite solar cells. *J. Mater. Chem. A* **2015**, *3*, 20305−20312.
(39) Anderson, T. W.; Pantoş, G. D.; Sanders, J. K. M. Supramolecular chemistry of monochiral naphthalenediimides. *Org. Biomol. Chem.* **2011**, *9*, 7547−7553.
(40) Zhao, Y.; Cotelle, Y.; Sakai, N.; Matile, S. Unorthodox Interactions at Work. *J. Am. Chem. Soc.* **2016**, *138*, 4270−4277.
(41) Suraru, S.-L.; Würthner, F. Strategies for the Synthesis of Functional Naphthalene Diimides. *Angew. Chem., Int. Ed.* **2014**, *53*, 7428−7448.
(42) Wang, S.; Pisula, W.; Müllen, K. Nanofiber growth and alignment in solution processed n-type naphthalene-diimide-based polymeric field-effect transistors. *J. Mater. Chem.* **2012**, *22*, 24827−24831.
(43) Shao, H.; Nguyen, T.; Romano, N. C.; Modarelli, D. A.; Parquette, J. R. Self-Assembly of 1-D n-Type Nanostructures Based on Naphthalene Diimide-Appended Dipeptides. *J. Am. Chem. Soc.* **2009**, *131*, 16374−16376.
(44) Basak, S.; Nanda, J.; Banerjee, A. Assembly of naphthalenediimide conjugated peptides: Aggregation induced changes in fluorescence. *Chem. Commun.* **2013**, *49*, 6891−6893.
(45) Basak, S.; Nandi, N.; Bhattacharyya, K.; Datta, A.; Banerjee, A. Fluorescence from an H-aggregated naphthalenediimide based peptide: Photophysical and computational investigation of this rare phenomenon. *Phys. Chem. Chem. Phys.* **2015**, *17*, 30398−30403.
(46) Bhosale, S. V.; Jani, C. H.; Langford, S. J. Chemistry of naphthalene diimides. *Chem. Soc. Rev.* **2008**, *37*, 331−342.
(47) Peebles, C.; Wight, C. D.; Iverson, B. L. Solution- and solid-state photophysical and stimuli-responsive behavior in conjugated monoalkoxynaphthalene−naphthalimide donor−acceptor dyads. *J. Mater. Chem. C* **2015**, *3*, 12156−12163.
(48) Kulkarni, C.; George, S. J. Carbonate Linkage Bearing Naphthalenediimides: Self-Assembly and Photophysical Properties. *Chem.—Eur. J.* **2014**, *20*, 4537−4541.
(49) Hong, Y.; Lam, J. W. Y.; Tang, B. Z. Aggregation-induced emission. *Chem. Soc. Rev.* **2011**, *40*, 5361−5388.
(50) Basak, S.; Nandi, N.; Baral, A.; Banerjee, A. Tailor-made design of J- or H-aggregated naphthalenediimide-based gels and remarkable fluorescence turn on/off behaviour depending on solvents. *Chem. Commun.* **2015**, *51*, 780−783.
(51) Sakai, N.; Mareda, J.; Vauthey, E.; Matile, S. Core-substituted naphthalenediimides. *Chem. Commun.* **2010**, *46*, 4225−4227.
(52) Görl, D.; Zhang, X.; Würthner, F. Molecular Assemblies of Perylene Bisimide Dyes in Water. *Angew. Chem., Int. Ed.* **2012**, *51*, 6328−6348.
(53) Nalluri, S. K. M.; Berdugo, C.; Javid, N.; Frederix, P. W. J. M.; Ulijn, R. V. Biocatalytic Self-Assembly of Supramolecular Charge-Transfer Nanostructures Based on n-Type Semiconductor-Appended Peptides. *Angew. Chem., Int. Ed.* **2014**, *53*, 5882−5887.
(54) Nandre, K. P.; Bhosale, S. V.; Krishna, K. V. S. R.; Gupta, A.; Bhosale, S. V. A phosphonic acid appended naphthalene diimide motif for self-assembly into tunable nanostructures through molecular recognition with arginine in water. *Chem. Commun.* **2013**, *49*, 5444−5446.
(55) Shao, H.; Seifert, J.; Romano, N. C.; Gao, M.; Helmus, J. J.; Jaroniec, C. P.; Modarelli, D. A.; Parquette, J. R. Amphiphilic Self-Assembly of an n-Type Nanotube. *Angew. Chem., Int. Ed.* **2010**, *49*, 7688−7691.
(56) Shao, H.; Gao, M.; Kim, S. H.; Jaroniec, C. P.; Parquette, J. R. Aqueous Self-Assembly of L-Lysine-Based Amphiphiles into 1D n-Type Nanotubes. *Chem.—Eur. J.* **2011**, *17*, 12882−12885.
(57) Shao, H.; Parquette, J. R. A π-conjugated hydrogel based on an fmoc-dipeptide naphthalene diimide semiconductor. *Chem. Commun.* **2010**, *46*, 4285−4287.
(58) Zhan, F.-K.; Hsu, S.-M.; Cheng, H.; Lin, H.-C. Remarkable influence of alkyl chain lengths on supramolecular hydrogelation of naphthalene diimide-capped dipeptides. *RSC Adv.* **2015**, *5*, 48961−48964.
(59) Liu, Y.-H.; Hsu, S.-M.; Wu, F.-Y.; Cheng, H.; Yeh, M.-Y.; Lin, H.-C. Electroactive Organic Dye Incorporating Dipeptides in the Formation of Self-Assembled Nanofibrous Hydrogels. *Bioconjugate Chem.* **2014**, *25*, 1794−1800.
(60) Hsu, L.-H.; Hsu, S.-M.; Wu, F.-Y.; Liu, Y.-H.; Nelli, S. R.; Yeh, M.-Y.; Lin, H.-C. Nanofibrous hydrogels self-assembled from naphthalene diimide (NDI)/amino acid conjugates. *RSC Adv.* **2015**, *5*, 20410−20413.
(61) Basu, K.; Baral, A.; Basak, S.; Dehsorkhi, A.; Nanda, J.; Bhunia, D.; Ghosh, S.; Castelletto, V.; Hamley, I. W.; Banerjee, A. Peptide based hydrogels for cancer drug release: Modulation of stiffness, drug release and proteolytic stability of hydrogels by incorporating D-amino acid residue(s). *Chem. Commun.* **2016**, *52*, 5045−5048.
(62) Jain, A.; George, S. J. New directions in supramolecular electronics. *Mater. Today* **2015**, *18*, 206−214.

DOI: 10.1021/acs.langmuir.6b02727
Langmuir 2016, 32, 13226−13233